AUTOPHAGY
2020, VOL. 16, NO. 11, 2017–2035
https://doi.org/10.1080/15548627.2020.1713643

Taylor & Francis
Taylor & Francis Group

RESEARCH PAPER

OPEN ACCESS Check for updates

Identification of the autophagy pathway in a mollusk bivalve, Crassostrea gigas

Sandy Picot[a], Nicole Faury[a], Isabelle Arzul[a], Bruno Chollet[a], Tristan Renault[b], and Benjamin Morga[a]

[a]SG2M-LGPMM, Laboratoire De Génétique Et Pathologie Des Mollusques Marins, Ifremer, La Tremblade, France; [b]Département Ressources Biologiques Et Environnement, Ifremer, Nantes, France

ABSTRACT

The Pacific oyster, *Crassostrea gigas*, is a mollusk bivalve commercially important as a food source. Pacific oysters are subjected to stress and diseases during culture. The autophagy pathway is involved in numerous cellular processes, including responses to starvation, cell death, and microorganism elimination. Autophagy also exists in *C. gigas*, and plays a role in the immune response against infections. Although this process is well-documented and conserved in most animals, it is still poorly understood in mollusks. To date, no study has provided a complete overview of the molecular mechanism of autophagy in mollusk bivalves. In this study, human and yeast ATG protein sequences and public databases (Uniprot and NCBI) were used to identify protein members of the *C. gigas* autophagy pathway. A total of 35 autophagy related proteins were found in the Pacific oyster. RACE-PCR was performed on several genes. Using molecular (real-time PCR) and protein-based (western blot and immunohistochemistry) approaches, the expression and localization of ATG12, ATG9, BECN1, MAP1LC3, MTOR, and SQSTM1, was investigated in different tissues of the Pacific oyster. Comparison with human and yeast counterparts demonstrated a high homology with the human autophagy pathway. The results also demonstrated that the key autophagy genes and their protein products were expressed in all the analyzed tissues of *C. gigas*. This study allows the characterization of the complete *C. gigas* autophagy pathway for the first time.

Abbreviations: ATG: autophagy related; Atg1/ULK: unc-51 like autophagy activating kinase; ATG7: autophagy related 7; ATG9: autophagy related 9; ATG12: autophagy related 12; BECN1: beclin 1; BSA: bovine serum albumin; cDNA: complementary deoxyribonucleic acid; DNA: deoxyribonucleic acid; GABARAP: GABA type A receptor-associated protein; IHC: immunohistochemistry; MAP1LC3/LC3/Atg8: microtubule associated protein 1 light chain 3; MTOR: mechanistic target of rapamycin kinase; NCBI: national center for biotechnology information; ORF: open reading frame; PBS: phosphate-buffered saline; PCR: polymerase chain reaction; PtdIns3K: class III phosphatidylinositol 3-kinase; RACE-PCR: rapid amplification of cDNA-ends by polymerase chain reaction; RNA: ribonucleic acid; SQSTM1: sequestosome 1; Uniprot: universal protein resource; WIPI: WD repeat domain, phosphoinositide interacting.

ARTICLE HISTORY
Received 2 April 2019
Revised 31 December 2019
Accepted 6 January 2020

KEYWORDS
Autophagy; autophagy related; *crassostrea gigas*; data mining; immunohistochemistry; real-time PCR; western blot

Introduction

Autophagy is an important mechanism that contributes to the maintenance of cellular homeostasis and different cellular processes, including adaptation to starvation, microorganism elimination, and cell death. Three main categories of autophagy are commonly described: microautophagy, chaperone-mediated autophagy, and macroautophagy [1,2]. During microautophagy, cytoplasmic compounds are taken up by invagination of the lysosomal membrane. In chaperone-mediated autophagy, the targeted proteins are translocated across the lysosomal membrane. Macroautophagy/autophagy acts as a bulk process that captures large portions of cytosol or sequesters organelles such as mitochondria or peroxisomes, which then fuse with lysosomes [1]. Each stage of the cellular mechanism of autophagy is regulated by several ATG (autophagy related) proteins.

The autophagy molecular pathway was first described in the yeast, *Saccharomyces cerevisiae*, in the 1990s [3]. Forty-two *ATG* have since been identified in yeast [4]. Since 1990, the research of *ATG* to better understand the autophagy molecular mechanism in other organisms has started. Homologs of *ATG* genes have been found in *Homo sapiens*, worms, flies, and mammals [1], and many have similar roles as in yeast [5]. The core molecular machinery of the autophagy pathway, which corresponds to ATG proteins essential for autophagosome formation [6,7], is highly conserved in eukaryotic cells including plants, yeast, and mammals [6,8–10]. In yeast, this core mechanism consists of 18 Atg proteins, classified into several functional groups: the Atg1/ULK (unc-51 like autophagy activating kinase) complex, class III phosphatidylinositol 3-kinase (PtdIns3K) complex, Atg12/ATG12 (autophagy related 12) and Atg8/LC3 (autophagy related 8/microtubule associated protein 1 light chain 3) conjugation systems, and Atg9/ATG9 (autophagy related 9) and its cycling system [5]. However, in many organisms, the molecular machinery of autophagy remains unknown.

CONTACT Benjamin Morga Benjamin.morga@ifremer.fr SG2M-LGPMM, Laboratoire De Génétique Et Pathologie Des Mollusques Marins, Ifremer, Avenue de Mus de Loup, La Tremblade 17390, France

Supplemental data for this article can be accessed here.

In mollusks, relatively few studies have aimed at identifying autophagy proteins and to analyze their responses in the presence of pathogens, or at different developmental stages. GABARAP (GABA type A receptor-associated protein) has been identified in the small abalone *Haliotis diversicolor*, and the relative expression of the relevant gene have been characterized at different stages of development or in presence of the bacteria, *Vibrio tapetis* [11]. In *C. gigas*, several ATG proteins, including MAP1LC3 (microtubule associated protein 1 light chain 3), BECN1 (beclin 1), ATG4 (autophagy related 4 cysteine peptidase), ATG5 (autophagy related 5), ATG7 (autophagy related 7), ATG9A (autophagy related 9A), and ATG16L1 (autophagy related 16 like 1) have been identified [12]; moreover, the relative expression of BECN1 and MAP1LC3 has been evaluated in presence of the virus *Ostreid herpesvirus* 1 (OsHV-1) [12]. However, the complete pathway has not been identified in bivalves.

Therefore, the aim of our study was to decipher the autophagy pathway in the Pacific oyster, *C. gigas*, the most important shellfish farming resource in France which has been affected by several diseases since the 1990s. Young and adult Pacific oysters have been regularly affected by outbreaks of mass mortality caused respectively by *Ostreid herpesvirus* 1 and the bacteria *Vibrio aestuarianus* [13]. The Pacific oyster genome was sequenced in 2012 [14], which allowed us to screen the Pacific oyster genes for the presence of ATG proteins. These sequences were then compared to ATG homolog present in others organisms. Some proteins were re-sequenced using rapid amplification of complementary deoxyribonucleic acid (cDNA)-ends by polymerase chain reaction (PCR) (RACE-PCR). The expression of the *ATG12, ATG9, BECN1, MAP1LC3A* (microtubule associated protein 1 light chain 3 alpha), *MTOR* (mechanistic target of rapamycin kinase), and *SQSTM1* (sequestosome 1) genes was detected in different tissues of *C. gigas* by real-time PCR. Finally, 4 human heterolog antibodies targeting BECN1, MAP1LC3A, MTOR, and SQSTM 1 were selected according to their high protein sequence homology with the *C. gigas* ATG counterparts, allowing us to confirm the presence of these 4 proteins in different tissues of *C. gigas* by western blotting and immunohistochemistry (IHC). In this study, we identified the ATG proteins in a mollusk bivalve, *C. gigas*, for the first time. Moreover, new protein-based and molecular approaches were described. These approaches can be used to further investigate the modulation of autophagy in *C. gigas* in response to various biotic and abiotic factors, including environmental stressors and pathogenic organisms.

Results

Protein mining of the C. gigas autophagy pathway

All the ATG protein sequences for *C. gigas, S. cerevisiae*, and *H. sapiens* were obtained (Fig. S1) and compared using the universal protein resource (Uniprot) and national center for biotechnology information (NCBI) databases. The results demonstrated that in *C. gigas*, 35 ATG proteins belonging to the 5 complexes implicated in initiation, nucleation, elongation, completion, and fusion of the autophagosome were identified (Tables 1–5).

As in other eukaryotes, the ATG proteins involved in the core molecular mechanism of autophagy are present in *C. gigas* and their amino acid sequences are conserved compared to *S. cerevisiae* and *H. sapiens*. The *C. gigas* LC3 family members GABARAP, GABARAPL2 (GABA type A receptor associated protein like 2), and MAP1LC3A share respectively, 93.9, 75, and 75% identity with the human counterpart sequences. The yeast counterpart sequences share respectively, 55.7 and 60.6% identity with the GABARAP and GABARAPL2 protein sequences of *C. gigas*. Most of the ATG proteins that constitute the 2 conjugation systems, ATG12 and LC3, as well as the Atg9/ATG9 system, appear to be well conserved between human and Pacific oyster. Several proteins of the Atg1/ULK and Ptdlns3K complexes of *C. gigas*, including MTOR (60.5%), PIK3C3 (phosphatidylinositol 3-kinase catalytic subunit type 3; 60.1%), and BECN1 (58.5%), share a high percentage of sequence identity with *H. sapiens* counterparts.

Nevertheless, several ATG proteins identified in *S. cerevisiae* or *H. sapiens* are not present in *C. gigas*. This is the case for Atg11, Atg17, Atg19, Atg20, Atg23, Snx4/Atg24, Atg27, Atg29, and Atg31 that are present only in yeast; and WIPI1 (WD repeat domain, phosphoinositide interacting 1) and MAP1LC3B (microtubule associated protein 1 light chain 3 beta), present only in *H. sapiens*.

Molecular characterization and phylogenetic analysis of key genes

Due to the importance of *ATG7, ATG9* and *ATG12* in the core molecular machinery of the autophagy pathway, the complete sequences of these 3 genes were obtained by 5′/3′ RACE-PCR and deposited in GenBank (Table 6).

The complete *ATG7* sequence (MK173046) contains 2334 nucleotides and 778 amino acids (Figure 1). We found an open reading frame (ORF) of 2091 nucleotides and 696 amino acids, containing the 2 entire ATG7_N and Apg7 domains (Figure 1A). The hypothetical isoelectric point is at 5.43 and the estimated molecular mass is 78.1 kDa. Nine homologous ATG7 protein sequences from different animals were used for multiple sequence alignments (Figure 1B). The results demonstrated that the 2 domain regions seem to be well conserved between all the species tested. The phylogenetic tree (Figure 1C) based on the ATG7 amino acid sequence from the same species showed that this protein is close to other mollusk species, and shares similarities with human ATG7 protein. *Crassostrea virginica* shares 85% identity (query cover of 99%) with our ATG7 sequence. Moreover, the *H. sapiens* ATG7 homolog shares 54% identity with *C. gigas* ATG7. The protein sequence seems to be different to other species like *C. elegans, D. melanogaster*, and *A. mellifera*.

The complete *ATG12* sequence (MK069431) comprises 309 amino acids and 929 nucleotides. This sequence presents one ORF of 357 bp and 118 amino acids, and contains the APG12 domain (Figure 2A). The hypothetical isoelectric point is at 6.72 and the estimated molecular mass is 13.1 kDa. Alignment of the protein sequences from ATG12 homolog species showed that the APG12 domain is highly conserved between all the tested species (Figure 2B). The phylogenetic tree showed that all the mollusks are classified in the same group

Table 1. List of the autophagy proteins involved in the Atg1/ULK kinase complex in the Pacific oyster (*C. gigas*) in comparison with the human (*Homo sapiens*) and yeast (*Saccharomyces cerevisiae*) proteins of the autophagy pathway.

Saccharomyces cerevisiae				Homo sapiens				Crassostrea gigas		
Name	*NCBI or Uniprot Accession number*	*% of identity in comparison with C. gigas*	*e-value*	*Name*	*NCBI or Uniprot Accession number*	*% of identity in comparison with C. gigas*	*e-value*	*Name*	*NCBI or Uniprot Accession number*	Domains of *C. gigas*
Tor1 (target of rapamycin 1)*	P35169	42.3	0.0	PREDICTED: *Homo sapiens* MTOR (mechanistic target of rapamycin kinase)*	XM_005263438.2	60.5	0.0	Serine/threonine-protein kinase TOR*	K1PYM7/ EKC29347	PIKKc_TOR, FAT, PI3Kc, TEL1
Tor2 (target of rapamycin 2)*	P32600	42.8	0.0					PREDICTED: *Crassostrea gigas* serine/ threonine-protein kinase MTOR (LOC105331599)*	XM_020068652.1	PIKKc_TOR, FAT, PI3Kc, TEL1
Atg1 (autophagy related 1)	P53104/ NM_001181045.1	-	-	ULK1 (unc-51 like autophagy activating kinase 1)	O75385	-	-	-	-	-
		34.1	2e-42	*Homo sapiens* ULK2 (unc-51 like autophagy activating kinase 2)	NM_001142610.2	47.3	6e-106	ULK2	K1PNL8/ EKC18065.1	STKc_UKL1_2-like, S_Tkc, Pkinase, SPS1
		34.1	7e-42	*Homo sapiens* ULK3 (unc-51 like kinase 3)	NM_001099436.4	49.7	3e-142	ULK3	K1Q313	STKc_ULK3, S_TKc, PKinase, SPS1*, MIT×3
		-	-	*Homo sapiens* ULK4 (unc-51 like kinase 4)	NM_017886.4	43.6	0.0	ULK4	K1QQA6	ATKc_ULK4, S_TKc, SPS1*, WSC×3
Atg13 (autophagy related 13)	Q06628	-	-	*Homo sapiens* ATG13 (autophagy related 13)	NM_001346354.1	36.5	1e-72	ATG13	K1QIF8/ XP_011420129.1	ATG13
Atg29 (autophagy related 29)	Q12092	-	-	-	-			-	-	-
Atg31 (autophagy related 31)	Q12421	-	-	-	-			-	-	-
Atg20 (autophagy related 20)	Q07528	-	-	-	-			-	-	-
Atg24/Snx4 (Sorting nexin 4)	P47057	-	-	-	-			-	-	-
-	-	-	-	*Homo sapiens* RB1CC1 (RB1 inducible coiled-coil 1)	XM_017014112.2	36.6	3e-41	RB1CC1	K1QSI9/ EKC24556.1	ATG11, Smc*, SMC_proK_A*
Atg17 (autophagy related 17)	Q06410	-	-	-	-	-	-	-	-	-
Atg11 (autophagy related 11)	Q12527	-	-	-	-	-	-	-	-	-
Atg19 (autophagy related 19)	P35193	-	-	-	-	-	-	-	-	-
-	-	-	-	ATG101 (autophagy related 101)	Q9BSB4/ NP_068753.2	62.8	7e-101	PREDICTED: *Crassostrea gigas* ATG101 (LOC105342150)	XM_011449015.2	ATG101
-	-	-	-	*Homo sapiens* ZFYVE1 (zinc finger FYVE-type containing 1)	NM_021260.4	54.1	0.0	ZFYVE1	K1QVT2/ EKC37743.1	GBP, FYVE_ZFYV1 × 2

(-) The protein is not present in this species. * Domain with incomplete sequence. * Sequence of *C. gigas* related to *H. sapiens* sequence. * Sequence of *C. gigas* related to *S. cerevisiae* sequence.

Table 2. List of the autophagy proteins involved in the Atg9/ATG9 complex in the Pacific oyster (*C. gigas*) in comparison with the human (*Homo sapiens*) and yeast (*Saccharomyces cerevisiae*) proteins of the autophagy pathway.

Saccharomyces cerevisiae				Homo sapiens				Crassostrea gigas		
Name	*NCBI or Uniprot Accession number*	*% of identity in comparison with C. gigas*	*e-value*	*Name*	*NCBI or Uniprot Accession number*	*% of identity in comparison with C. gigas*	*e-value*	*Name*	*NCBI or Uniprot Accession number*	Domains of *C. gigas*
Atg9 (autophagy related 9)	Q12142	30.1	2e-29	ATG9A (autophagy related 9A)	Q7Z3C6	42.1	1e-128	PREDICTED: *Crassostrea gigas* ATG9A (LOC105320700)	XM_011418747.2	APG9
		-	-	ATG9B (autophagy related 9B)	Q674R7	-	-	-	-	-
Atg18 (autophagy related 18)	P43601/ NM_001179986.1	-	-	WIPI1 (WD repeat domain, phosphoinositide interacting 1)	Q5MNZ9	-	-	-	-	-
		37.2	3e-23	*Homo sapiens* WIPI2 (WD repeat domain, phosphoinositide interacting 2)	NM_001033518.2	60.5	6e-180	WIPI2	K1QZR2/ EKC39143.1	WD40*
		28.9	1e-35	*Homo sapiens* WDR45B/WIPI3 (WD repeat domain 45B)	KX434429.1	73.1	0.0	WIPI3	K1PZL8/ XM_011447404.2	WD40*
		27.38	2e-31	WDR45/WIPI4 (WD repeat domain 45)	Q9Y484	61.1	5e-161	PREDICTED: *Crassostrea gigas* WIPI4-like (LOC105347054)	XM_011455938.2	WD40*
Atg2 (autophagy related 2)	P53855/ NM_001183080.1*	31.1	2e-11	*Homo sapiens* ATG2A (autophagy related 2A)	NM_015104.3	45	8e-134	ATG2A-like	K1RSP2/ EKC37546.1	VPS13_C*, ATG2_CAD
		31.2	6e-12	PREDICTED: *Homo sapiens* ATG2B (autophagy related 2B) *	XM_006720187.2	33.7	7e-96	ATG2B-like*	K1QL77/ EKC37547.1	Chorein_N, MRS6
								PREDICTED: *Crassostrea gigas* ATG2B (LOC105338878)*	XM_011444166.2	Chorein_N, MRS6*, ATG2_CAD, ATG_C, VPS13_C*
Atg23 (autophagy related 23)	Q06671	-	-	-	-	-	-	-	-	-
Atg27 (autophagy related 27)	P46989	-	-	-	-	-	-	-	-	-

(-) The protein is not present in this species. * Domain with incomplete sequence.* Sequence of *C. gigas* related to *H. sapiens* sequence. * Sequence of *C. gigas* related to *S. cerevisiae* sequence.

Table 3. List of the autophagy proteins involved in the PtdIns3K complex in the Pacific oyster (*C. gigas*) in comparison with the human (*Homo sapiens*) and yeast (*Saccharomyces cerevisiae*) proteins of the autophagy pathway.

Saccharomyces cerevisiae				Homo sapiens				Crassostrea gigas		
Name	*NCBI or Uniprot Accession number*	*% of identity in comparison with C. gigas*	*e-value*	*Name*	*NCBI or Uniprot Accession number*	*% of identity in comparison with C. gigas*	*e-value*	*Name*	*NCBI or Uniprot Accession number*	Domains of *C. gigas*
Saccharomyces cerevisiae S288C Vps34 (vacuolar protein sorting 34)	NM_001182127.1	33.6	2e-159	*Homo sapiens* PIK3C3 (phosphatidylinositol 3-kinase catalytic subunit type 3)	NM_002647.4	60.1	0.0	PIK3C3	K1PVC2/ EKC20235.1	C2_PI3K_Class_III, PI3K_C2, PI3Ka_III, PI3Kc_III, PI3Kc, PI3_PI4_kinase
Saccharomyces cerevisiae Vps15 (vacuolar protein sorting 15)	NM_001178445.2	39.6	2e-70	*Homo sapiens* PIK3R4 (phosphoinositide-3-kinase regulatory subunit 4)	NM_014602.3	50.2	0.0	PIK3R4	K1R976/ XP_011416324.1	STKc_Vps15, SPS1, WD40
Saccharomyces cerevisiae S288C Vps30 (vacuolar protein sorting 30)	NM_001183934.1	27.3	1e-32	*Homo sapiens* BECN1 (beclin 1)	AF139131.1	58.5	1e-173	BECN1	K1QHY7	APG6, BH3
Atg14 (autophagy related 14)	P38270	-	-	ATG14 (autophagy related 14)	Q6ZNE5	34.5	4e-63	PREDICTED: *Crassostrea gigas*ATG14 (LOC105344371)	XM_011452143.2	ATG14, PTZ00121*
-	-	-	-	*Homo sapiens* AMBRA1 (autophagy and beclin 1 regulator 1)	DQ870924.1	45.6	3e-56	AMBRA1	K1QU33/ EKC40357.1	WD40*
Vps38 (vacuolar protein sorting 38)	Q05919	-	-	UVRAG (UV radiation resistance-associated)	Q9P2Y5	36.1	7e-62	PREDICTED: *Crassostrea gigas* UVRAG (LOC105334521)	XM_020069853.1	Atg14
-	-	-	-	RUBCN (rubicon autophagy regulator)	Q92622	32.4	4e-100	PREDICTED: *Crassostrea gigas* RUBCN (LOC105322496)	XM_011421238.2	RUN, zf-RING_9*
-	-	-	-	*Homo sapiens* SH3GLB1 (SH3 domain containing GRB2 like, endophilin B1)	AF263293.1	55.2	8e-148	SH3GLB1	K1Q963	BAR_Endophilin_B, SH3_Endophilin_B

(-) The protein is not present in this species. * Domain with incomplete sequence.

Table 4. List of the autophagy proteins involved in the ATG12 conjugation system in the Pacific oyster (*C. gigas*) in comparison with the human (*Homo sapiens*) and yeast (*Saccharomyces cerevisiae*) proteins of the autophagy pathway.

Saccharomyces cerevisiae				Homo sapiens				Crassostrea gigas		
Name	*NCBI or Uniprot Accession number*	*% of identity in comparison with C. gigas*	*e-value*	*Name*	*NCBI or Uniprot Accession number*	*% of identity in comparison with C. gigas*	*e-value*	*Name*	*NCBI or Uniprot Accession number*	Domains of *C. gigas*
Atg12 (autophagy related 12)	P38316	29.8	3e-09	ATG12 (autophagy related 12)	O94817	63.1	5e-40	PREDICTED: *Crassostrea gigas* ATG12 (LOC105320040)	XM_011417800.2	APG12, Ubl_ATG12
Saccharomyces cerevisiae S288C Atg5 (autophagy related 5)	NM_001183963.1	24.3	4e-08	*Homo sapiens* ATG5 (autophagy related 5)	EU283339.1	52.4	1e-102	ATG5	K1RAJ5	APG5
Atg16 (autophagy related 16)	Q03818	-	-	*Homo sapiens* ATG16L1 isoform 2 (autophagy related protein 16 like 1)	JQ924062.1	43.5	6e-139	ATG16	K1RWG6	ATG16, WD40 × 3, WD40*, Smc*
		-	-	Human ATG16L2 (autophagy related 16 like 2)	Q8NAA4	-	-	-	-	-
Atg10 (autophagy related 10)	Q07879	-	-	PREDICTED: *Homo sapiens* ATG10 (autophagy related 10)	XM_005248611.5	48.3	5e-36	ATG10	K1PT50	Autophagy_act_C

(-) The protein is not present in this species. * Domain with incomplete sequence.

Table 5. List of the autophagy proteins involved in the LC3 conjugation system in the Pacific oyster (*C. gigas*) in comparison with the human (*Homo sapiens*) and yeast (*Saccharomyces cerevisiae*) proteins of the autophagy pathway.

Saccharomyces cerevisiae				Homo sapiens				Crassostrea gigas		
Name	*NCBI or Uniprot Accession number*	*% of identity in comparison with C. gigas*	*e-value*	*Name*	*NCBI or Uniprot Accession number*	*% of identity in comparison with C. gigas*	*e-value*	*Name*	*NCBI or Uniprot Accession number*	Domains of *C. gigas*
Atg8 (autophagy related 8)	P38182/ NM_001178318.1	35.2	1e-20	*Homo sapiens* MAP1LC3A (microtubule associated protein 1 light chain 3 alpha)	BT007452.1	75	1e-61	MAP1LC3A	K1R9V4/XP 011447694.1	GABARAP, Atg8
		-	-	MAP1LC3B (microtubule associated protein 1 light chain 3 beta)	Q9GZQ8	-	-	-	-	-
		37.3	8e-22	PREDICTED: *Homo sapiens* MAP1LC3C (microtubule associated protein 1 light chain 3 gamma)	XM_005273139.3	67.7	4e-53	MAP1LC3C	K1QLL7/ XP_011415834.1	GABARAP, Atg8, PTZ00380
		55.7	3e-44	*Homo sapiens* GABARAP (GABA type A receptor-associated protein)	AF161586.1	93.9	2e-73	GABARAP	K1PXH7/ XP_011437796.1	GABARAP, Atg8, PTZ00380
		-	-	GABARAPL1 (GABA type A receptor-associated protein like 1)	Q9H0R8	-	-	-	-	-
		60.6	2e-48	*Homo sapiens* GABARAPL2 (GABA type A receptor associated protein like 2)	NM_007285.7	75	2e-57	GABARAPL2	K1QQ43/ XP_011432603.1	GABARAP, Atg8, PTZ00380
		-	-	GABARAPL3 (GABA type A receptor associated protein like 3 pseudogene)	Q9BY60	-	-	-	-	-
Atg7 (autophagy related 7)*	P38862	46.9	3e-125	ATG7 (autophagy related 7)*	O95352	52.1	0.0	PREDICTED: *Crassostrea gigas* ATG7 (LOC105321294)*	XM_011419559.2	ATG7_N, Apg7, ThiF*, E1_like_apg7, PRK05600*
								PREDICTED: *Crassostrea gigas* ATG7 (LOC105340241)*	XM_020072211.1	ATG7_N*, Apg7, ThiF*, E1_like_apg7*, PRK05600*
Saccharomyces cerevisiae S288C Atg3 (autophagy related 3)	NM_001183184.3	31.5	1e-40	*Homo sapiens* ATG3 (autophagy related 3)	AB079384.1	65.7	5e-147	ATG3	K1R934	Autophagy_N, Autophagy_act_C, Autophagy_
Saccharomyces cerevisiae S288C Atg4 (autophagy related 4)	P53867/ NM_001183061.1	-	-	ATG4A (autophagy related 4A cysteine peptidase)	Q8WYN0	-	-	-	-	-
		33.6	2e-07	PREDICTED: *Homo sapiens* ATG4B (autophagy related 4B cysteine peptidase)	XM_017003638.1	45.3	1e-103	ATG4 cysteine protease	K1QKP1	Peptidase_C54
		29.12	7e-34	ATG4C (autophagy related 4C cysteine peptidase)	Q96DT6	37.4	3e-99	PREDICTED: *Crassostrea gigas* ATG4C-like (LOC105336676)	XM_011441099.2	Peptidase_C54
		-	-	ATG4D (autophagy related 4D cysteine peptidase)	Q86TL0	-	-	-	-	-
-	-	-	-	SQSTM1 (sequestosome 1)	Q13501	32.8	3e-54	PREDICTED: *Crassostrea gigas* SQSTM1 (LOC105345634)	XM_011453843.2	PB1 × 2, ZZ_NBR1_like, ZnF_ZZ, ZZ, UBA-SQSTM

(-) The protein is not present in this species. * Domain with incomplete sequence. * Sequence of *C. gigas* related to *H. sapiens* sequence. * Sequence of *C. gigas* related to *S. cerevisiae* sequence.

Table 6. Gene sequences obtained by RACE-PCR from autophagy genes *ATG7, ATG12*, and *ATG9* in hemocytes of *C. gigas*.

Gene name	Gene Length	Protein length	GenBank accession	Identity with *H. sapiens*	Identity with *S. cerevisiae*	Isoelectric point	Molecular weight	Sequence RACE
ATG7	2334	696	MK173046	54%	39%	5.43	78.1 kDa	3′GGACTATCCAGGCTGGCCTCTTAGG 5′GGGGGCAGACAAAGTCTTTACTCAGG
ATG12	929	118	MK069431	62%	19%	6.72	13.1 kDa	3′ACCAGCTGGAGATGCTCCAATTATGA 5′GTTTTCCATCACTCCCAAAGCAATCA
ATG9	3032	1010	MK069430	43%	19%	5.88	91.9 kDa	3′GCTCCTTTTATCTCACTGCCCTCCAC 5′CCGGTGGTATATGTCCAGCTCTGT

The percentage of identity were obtained by alignment of amino acid sequences.

(Figure 2C). This sequence shares high identity with *C. virginica* (94%, query cover of 100%). The *C. gigas* sequence is more similar to the *H. sapiens* than the *C. elegans* and *S. purpuratus* sequences. The *H. sapiens* sequence shares 62% identity with *C. gigas*.

The sequence of *ATG9* (MK069430) comprises 3032 nucleotides and 1010 amino acids. One ORF was found, consisting of 2409 nucleotides and 802 amino acids, and contains the entire APG9 domain (Figure 3A). The hypothetical isoelectric point is at 5.88 and the estimated molecular mass is 91.9 kDa. Sequence alignment of the ATG9 protein of different species showed that the APG9 domain is highly conserved (Figure 3B). The phylogenetic tree demonstrated that the *C. gigas* ATG9 sequence is similar to bivalves and brachiopods, like those from *C. virginica* (88%, query cover of 97%) and *Lingula anatina* (52%, query cover of 99%). This sequence is also similar to vertebrates. *H. sapiens* ATG9A shares 43% identity with *C. gigas* (Figure 3C).

The *ULK2* (unc-51 like autophagy activating kinase 2) sequence was identified in *C. gigas* (Uniprot number: K1PNL8). This sequence consists of 2808 nucleotides and 936 amino acids, and contains the entire STKc_ULK1_2-like domain (Figure 4A). The hypothetical isoelectric point is at 8.64 and the estimated molecular mass is 103 kDa. The alignment of eight protein sequences from different organisms demonstrated that the STKc_ULK1_2-like domain situated in the first part of the sequence seems to be well conserved between the different species (Figure 4B). The phylogenetic tree showed that the ULK2 sequence is similar to vertebrate ULK2 sequences (Figure 4C). The *H. sapiens* sequence shares 34% identity with the *C. gigas* sequence, and our sequence shares a high identity with other bivalve and brachiopod ULK2 proteins, like those from *C. virginica* (94%, query cover 100%), and *L. anatina* (50%, query cover 99%).

Expression of 6 ATG genes in C. gigas tissues

The relative expression of key *ATG* genes of the 2 initiation complexes (*MTOR* and *BECN1*), the LC3 and ATG12 conjugation systems (*ATG12, SQSTM1* and *MAP1LC3A*) and the Atg9/ATG9 cycling system (*ATG9*) was measured to determine in which *C. gigas* tissues autophagy occurs. All the tissues tested constitutively expressed *ATG12, ATG9, BECN1, MTOR, SQSTM1*, and *MAP1LC3A* (Figure 5). However, the level of expression of each gene varied among the analyzed tissues.

Detection of autophagy proteins in C. gigas

Western blotting and IHC approaches were used to confirm the presence of key ATG proteins of the 2 initiation complexes (MTOR and BECN1) and the LC3 conjugation system (SQSTM1 and MAP1LC3) in *C. gigas* tissues.

The western blot analysis revealed that the autophagy proteins BECN1, MAP1LC3, MTOR, and SQSTM1 were abundant in all the tested tissues of the Pacific oyster (Figure 6). While MAP1LC3-I appeared to be expressed in all the tissues tested, the MAP1LC3-II form was strongly detected in the mantle and gills.

The IHC results obtained from *C. gigas* tissues confirmed the results obtained by western blot and allowed to better detect the localization of autophagy proteins in the tissues (Figure 7). No labeling was observed in the negative control *C. gigas* tissues (Figure 7A–F). In contrast, in the presence of the 4 primary antibodies, labeling (corresponding to the formation of brown precipitates) was observed in the mantle, gills, gonad, and digestive gland. Each protein exhibited a specific localization pattern. The SQSTM1 protein was detected in the epithelium of the mantle and gills (Figure 7G,I), nervous tissue, connective tissue (Figure 7H), and glandular cells of the digestive tubules (Figure 7J). Spots of strong MAP1LC3A staining were observed in vesicular cells of connective tissue, mantle (Figure 7K), and digestive epithelium (Figure 7M). A diffuse labeling was observed in muscular fibers (Figure 7L) and in granular cells of the digestive tubules (Figure 7N). For the BECN1 protein, positive staining was observed in glandular cells of the digestive tubules (Figure 7R), some cells of the gill filament (Figure 7Q), nervous tissue (Figure 7O), and mantle and gonad epithelia (Figure 7P). MTOR-specific antibodies stained the muscle, nervous tissue, and some nuclei of mantle epithelial cells (Figure 7S), connective tissue in gills and gonad (Figure 7U,T), nuclei of oocytes, and glandular cells in the digestive tubules (Figure 7V).

Discussion

Macroautophagy, more commonly called autophagy, is a mechanism widely conserved in eukaryotes and has been described for model organisms like yeast, humans, worms, and insects [1,9]. However, in many organisms like mollusks, autophagy is still poorly understood. Although several ATG proteins have been reported in mollusks, information on the components of the molecular machinery of the autophagy pathway in this phylum remains scarce. Moreover, the localization of autophagy activity in bivalve tissues has not been explored.

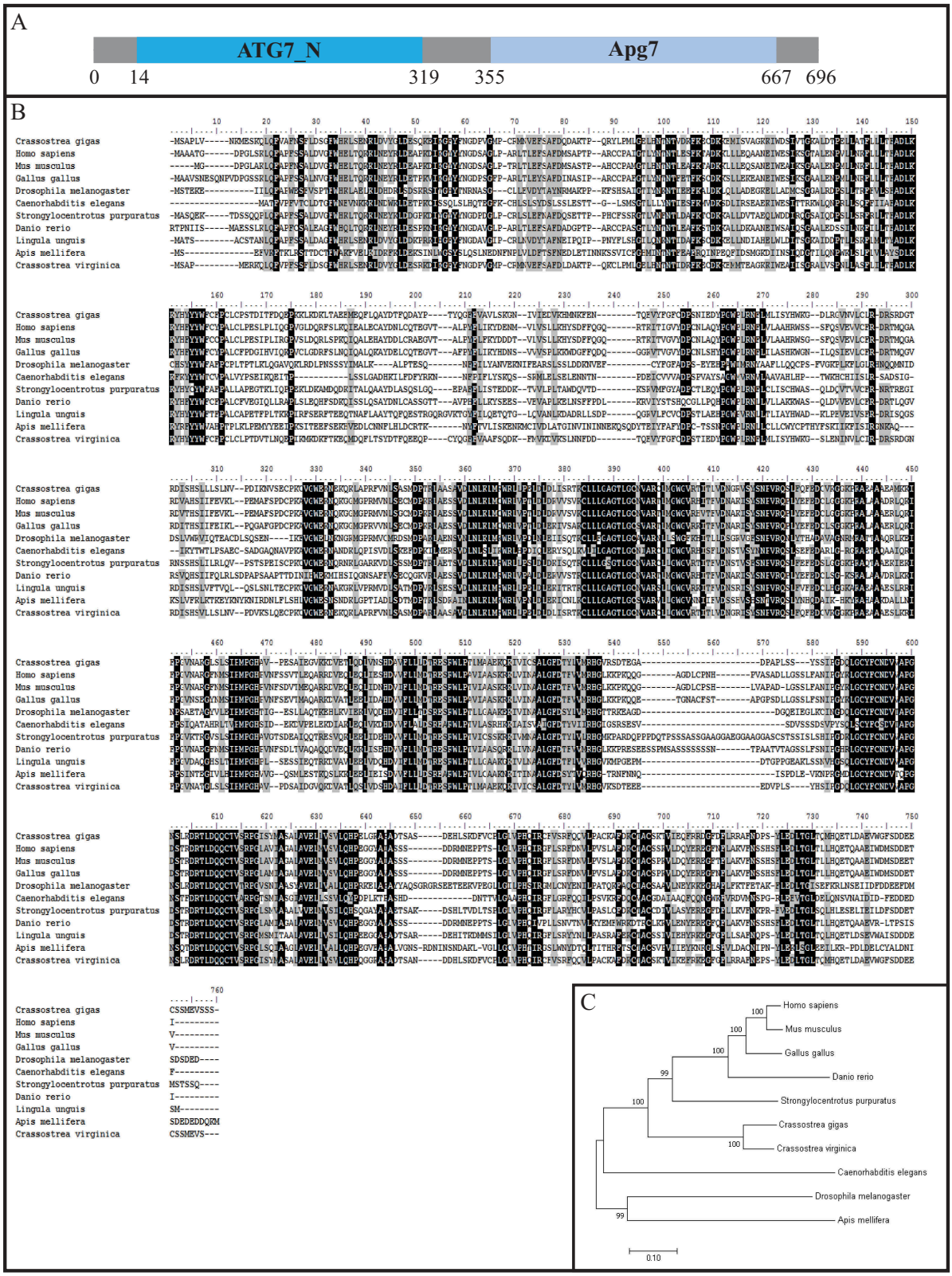

Figure 1. Phylogenetic analysis of autophagy protein ATG7 of the Pacific oyster. (A) Schematic annotation of the ORF protein sequence. (B) Global alignment of counterpart proteins sequences of ATG7 from animals of different part of the animal kingdom. Dashes (-) indicate gaps. (C) Neighbor-joining tree (bootstrap = 1000 replications) of the different autophagy proteins.

Mollusk bivalves are generally exposed to numerous biotic (pathogens) and abiotic (tide, pollution) stressors. Initial studies demonstrated that the autophagy pathway can play an important role in the response to these different stress factors [12,15–17], highlighting the importance of elucidating the autophagy pathway in bivalve mollusks. In this study, we identified the autophagy pathway by data mining of the Pacific oyster genome [14]. Real-time quantitative PCR,

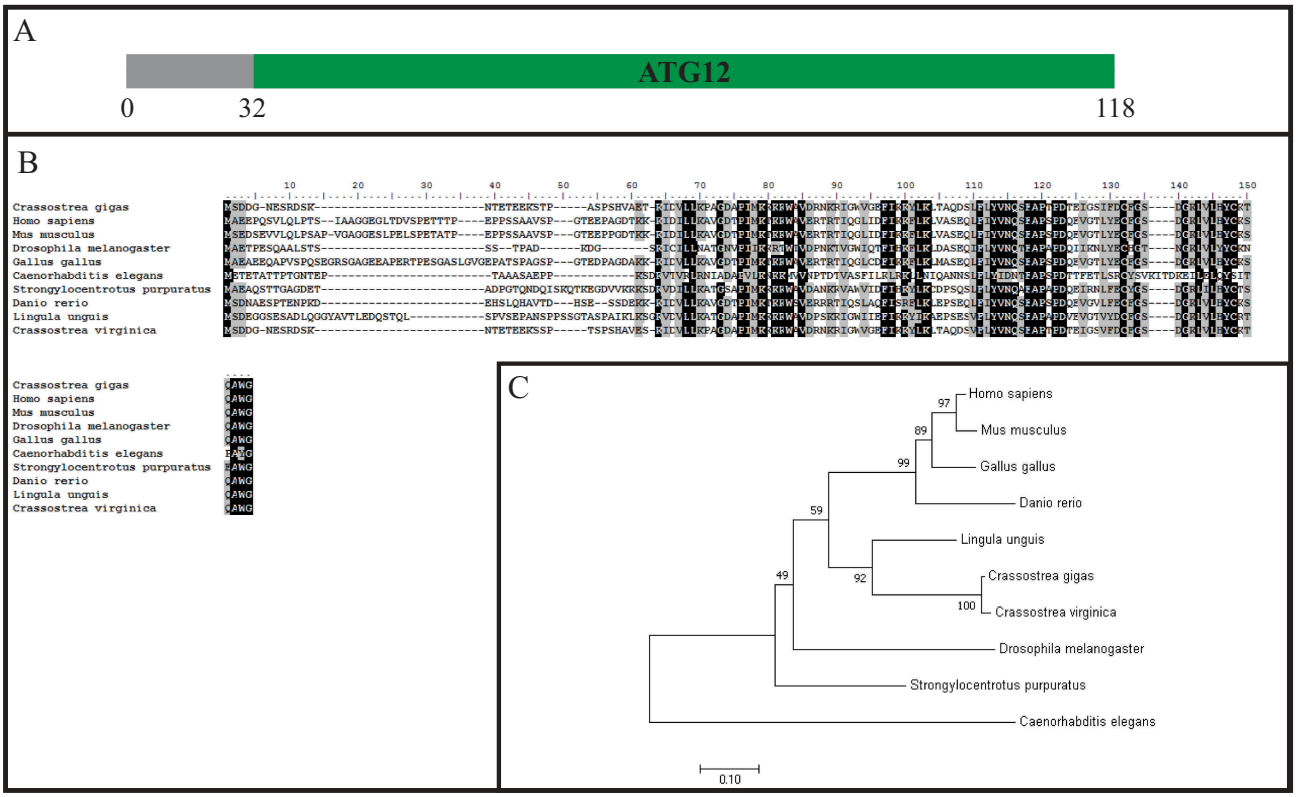

Figure 2. Phylogenetic analysis of autophagy protein ATG12 of the Pacific oyster. (A) Schematic annotation of the ORF protein sequence. (B) Global alignment of counterpart proteins sequences of ATG12 from animals of different part of the animal kingdom. Dashes (-) indicate gaps. (C) Neighbor-joining tree (bootstrap = 1000 replications) of the different autophagy proteins.

western blotting, and IHC were used to study the ATG proteins that constitute the *C. gigas* autophagy pathway, and the expression of 6 key genes and 4 proteins were analyzed in different tissue compartments of the Pacific oyster.

The core molecular machinery of autophagy comprises 5 complexes containing ATG proteins conserved from yeast to mammals [5,7]. Our results showed that the major ATG proteins and the different complexes of the core molecular machinery are present and expressed in the Pacific oyster (Figure 8). The autophagy pathway in *C. gigas* is conserved among eukaryotes, from the initiation of autophagy by ULK and the PtdIns3K complex to autophagosome formation by the Atg9/ATG9 cycling system and 2 conjugation systems, ATG12 and LC3.

Our results also showed conserved sequences and conserved domains in some proteins of the autophagy pathway. Several key ATG proteins of the 2 complexes of the initiation step (BECN1 and ULK2) and the LC3 conjugation system (GABARAP and LC3 family members, SQSTM1) were highly conserved. BECN1 plays a role as a platform for assembly and stimulation of activity [18], whereas ULK2 mediates membrane targeting, vesicle tethering, and co-assembly of subunits [19–21]. LC3 family members and SQSTM1 are important for membrane isolation during the elongation step [22] and cargo recognition of polyubiquitinated proteins, respectively [23–26]. Except for ULK2, the domains that comprise these proteins are the same as for their *H. sapiens* counterparts [18,22,27,28]. These data suggest that the role of these proteins is conserved between mollusks and mammals. In support of these results, the ATG proteins BECN1 and MAP1LC3 were reported to be phylogenetically close to their human orthologs [12]. Moreover, higher eukaryotes of different phyla (worms, insects, plants, mammals) have essentially similar roles compared to yeast [9,29].

Some other *C. gigas* ATG protein sequences were incomplete and some were not found. The sequences of several proteins implicated in the core molecular machinery of autophagy were incomplete. However, these proteins that are conserved in other invertebrates like the crustacean *Macrobrachium rosenbergii* [10], play important roles in the mechanism of autophagy. In our study, we obtained the complete sequences for *ATG7, ATG12*, and *ATG9* by RACE-PCR. The amino acid sequences of these 3 proteins are highly conserved with their eukaryotic counterparts. Moreover, the domains are also conserved and similar to *H. sapiens* protein counterparts, suggesting a conserved function for these proteins as with the other eukaryotes. ATG7 and ATG12 mediate the tethering of a phosphatidylethanolamine on the MAP1LC3 protein, and ATG9 regulates/participates in the delivery of membrane for the formation of autophagosomes [7,30]. The full characterization of *ATG7, ATG12* and *ATG9* by RACE-PCR demonstrated that the genome assembly of *C. gigas* by Zhang *et al.* [14] is not reliable or have annotation problems.

We did not find MAP1LC3B, ULK1 (unc-51 like autophagy activating kinase 1), and WIPI1 protein in *C. gigas*.

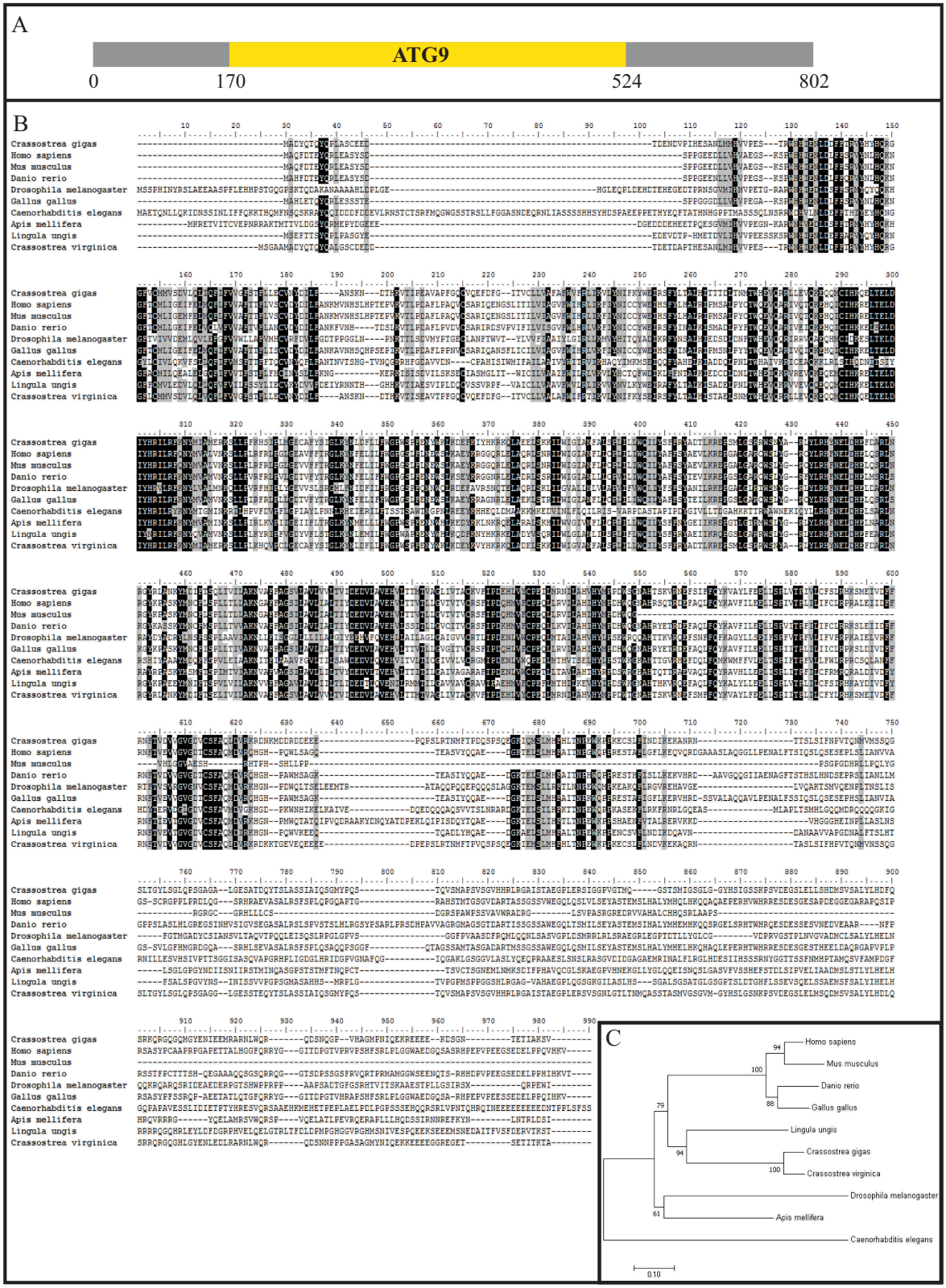

Figure 3. Phylogenetic analysis of autophagy protein ATG9 of the Pacific oyster. (A) Schematic annotation of the ORF protein sequence. (B) Global alignment of counterpart proteins sequences of ATG9 from animals of different part of the animal kingdom. Dashes (-) indicate gaps. (C) Neighbor-joining tree (bootstrap = 1000 replications) of the different autophagy proteins.

Nevertheless, these proteins play important roles in the mechanisms of autophagy [31–33]. MAP1LC3B is the more commonly described and studied LC3 and GABARAP family member [33]. Schaaf [33] reported that this protein is implicated in phagophore elongation, promotes tethering and membrane fusion. ULK1 is involved in the phosphorylation of BECN1, activation of the PtdIns3K complex, and promotion of autophagy [34]. WIPI1 is known to play an

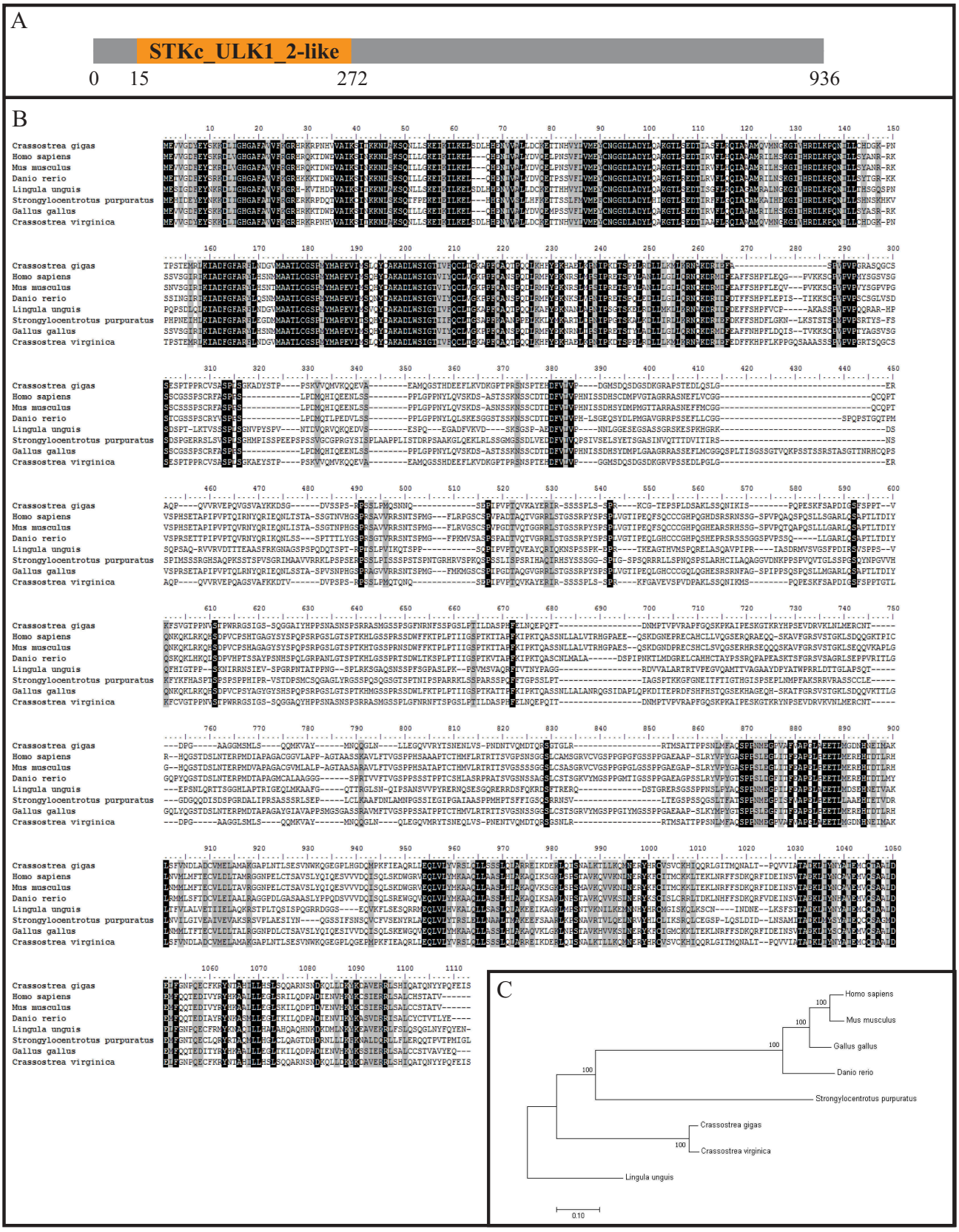

Figure 4. Phylogenetic analysis of autophagy protein ULK2 of the Pacific oyster. (A) Schematic annotation of the ORF protein sequence. (B) Global alignment of counterpart proteins sequences of ULK2 from animals of different part of the animal kingdom. Dashes (-) indicate gaps. (C) Neighbor-joining tree (bootstrap = 1000 replications) of the different autophagy proteins.

essential function in mammals [32]. Meanwhile, WIPI1, WIPI2 (WD repeat domain, phosphoinositide interacting 2), and WDR45/WIPI4 (WD repeat domain 45) are redundant phosphatidylinositol 3-phosphate (PtdIns3P) downstream effectors of PIK3C3-mediated phosphatidylinositol 3-phosphate production at the onset of autophagy [32].

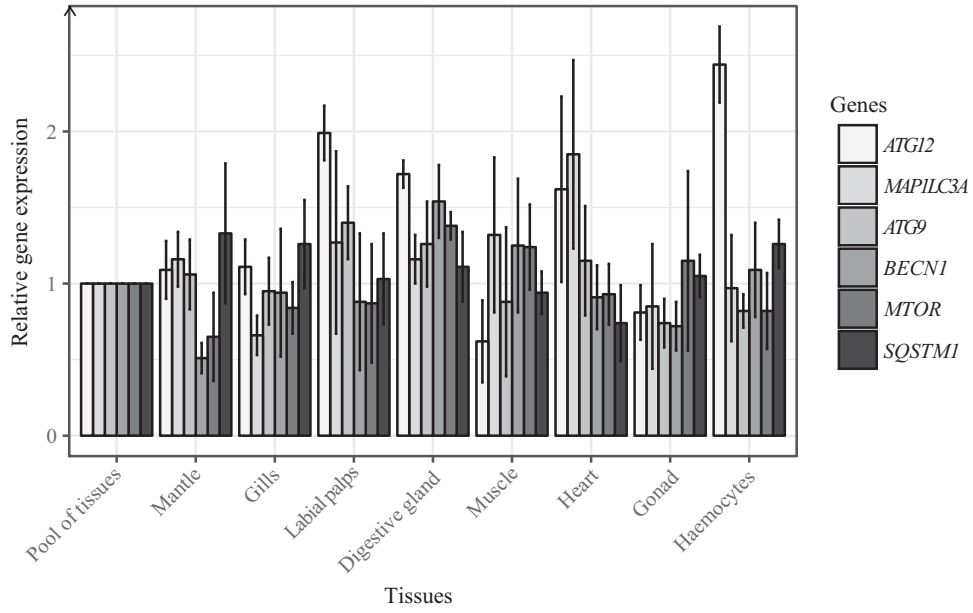

Figure 5. Relative gene expression of *ATG12, ATG9, BECN1, MTOR, SQSTM1* and *MAP1LC3A* in different tissues of *Crassostrea gigas* by real-time PCR. Error bars represent standard deviations.

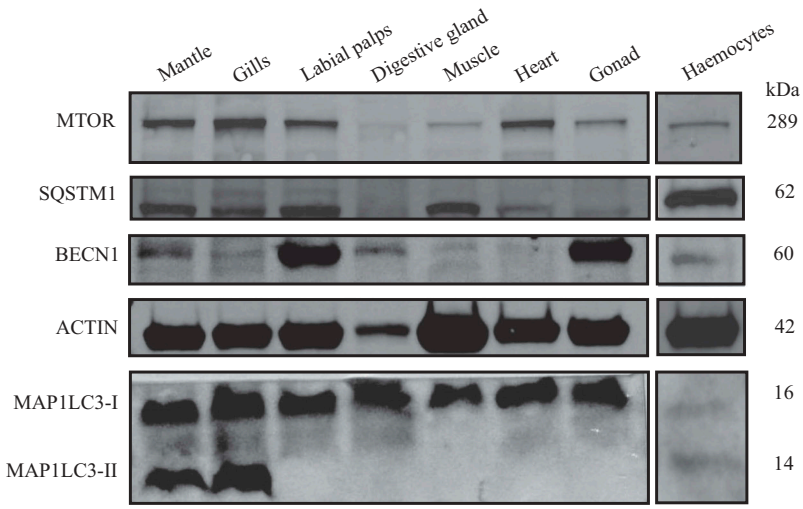

Figure 6. Detection of the protein BECN1, MTOR, SQSTM1 and MAP1LC3 in different tissues of *Crassostrea gigas*.

Nevertheless, the specific role of each ULK1 homolog and each WIPI, LC3 and GABARAP families members remains unclear [22,32,35]. We do not know if the absence of these proteins can affect the autophagy machinery, or if their function is replaced by redundancy with other family members. In addition, we cannot conclude whether the proteins are simply not present in *C. gigas*, or whether the absence is due to issues with the annotation or assemblage of the *C. gigas* genome.

Moreover, other Atg proteins (Atg11, Atg17, Atg19, Atg20, Atg23, Atg24, Atg27, Atg29, and Atg31) specific to other autophagy-related pathways defined in yeast (starvation-induced autophagy, cytoplasm-to-vacuole targeting, and pexophagy pathways) [36] were not found in *C. gigas*. These proteins are not essential for the functioning of the core molecular machinery and are not required for the formation of the autophagosome [36].

Using real-time PCR, western blotting, and IHC, we detected the expression of 6 genes (*ATG12, ATG9, MTOR, SQSTM1, BECN1*, and *MAP1LC3A*) and 4 proteins (MTOR, SQSTM1, BECN1, and MAP1LC3A) in different tissues of the Pacific oyster. According to the real-time PCR results, *ATG12, ATG9, MAP1LC3A, SQSTM1, MTOR*, and *BECN1* were constitutively expressed in the mantle, gills, muscle, labial palps, digestive gland, gonad, heart, and hemolymph at the gene level. Western blotting results demonstrated that MAP1LC3A, SQSTM1, MTOR, and BECN1 were also constitutively expressed in all these tissues at the protein level. Similar results were obtained for the abalone *Haliotis diversicolor* for saGABARAP [11]. The presence of the

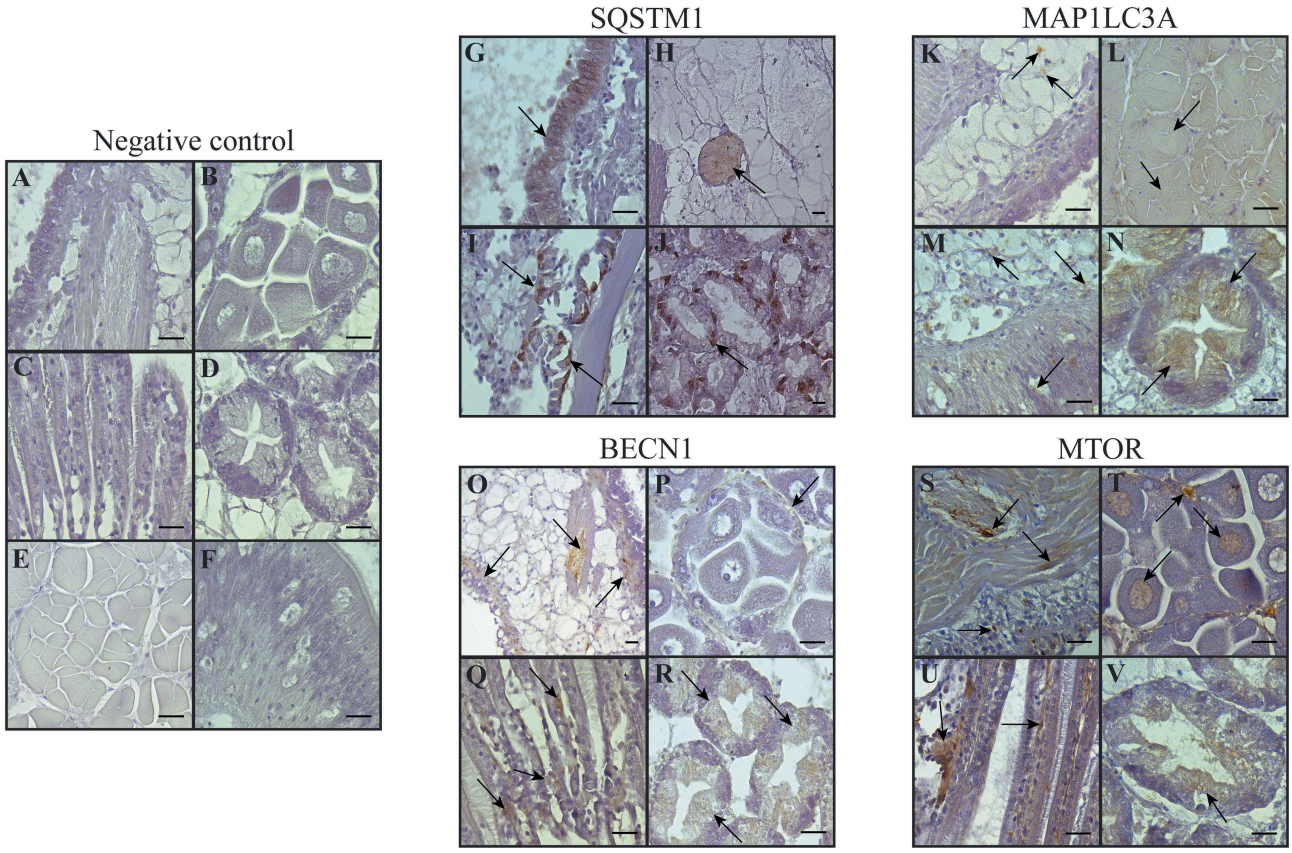

Figure 7. Immunohistochemical detection of BECN1, MTOR, SQSTM1 and MAP1LC3A in several tissues of the Pacific oyster, *Crassostrea gigas*. (A) Mantle with connective tissue, nerf and muscle, (B) gonad, (C) gills, (D) digestive tubules, (E) muscle, (F) digestive gland epithelium, (G) mantle with connective tissue, (H) nerf in the mantle connective tissue, (I) gills, (J) digestive tubules, (K) mantle with connective tissue, (L) muscle, (M) digestive gland epithelium and connective tissue, (N) digestive tubule, (O) mantle with connective tissue, nerf and muscle, (P) gonad, (Q) gills, (R) digestive tubules, (S) mantle with nerf and muscle, (T) gonad, (U) gills and (V) digestive tubule. Scale bar: 20 µm.

MAP1LC3, SQSTM1, and BECN1 proteins was also detected by western blot in various tissues of the giant freshwater prawn *M. rosenbergii* including the hepatopancreas, ovary, muscle, brain, eyestalk, and thoracic glands [10]. More generally it is know that autophagy occurs at a basal level in mammalian systems [37]. A basal level of autophagy is active in most cells type where it is postulated to play a housekeeping role in maintaining the integrity of intracellular organelles and proteins [1,38].These results suggest that, in *C. gigas*, autophagy play a role in important cellular processes as homeostasis by allowing a constitutive cytosolic components turnover. However, at the protein level, the MAP1LC3-II form is detected only in the mantle, gills and the hemocytes of *C. gigas*. The amount of MAP1LC3-II (the lapidated form of MAP1LC3-I), is closely correlated with the number of autophagosomes, serving as a good monitoring indicator of autophagosome formation [39]. Some authors have already reported that MAP1LC3-II amounts are tissues or cells context dependent [40,41]. Moreover, the conversion of MAP1LC3-I in MAP1LC3-II form depend of the cell type and of the kind of stress to which cells are subjected [42]. In *C. gigas*, it could be supposed that the MAP1LC3-II amount is tissue dependent.

The IHC analysis using the 4 antibodies revealed diffuse staining in the mantle, gills, gonad, and digestive gland of the Pacific oyster, *C. gigas*. This phenomenon has been frequently reported for mammal tissues labeled with MAP1LC3 and BECN1-specific antibodies [42,43]. With IHC, a diffuse staining is more commonly observed in tissues than a characteristic spot staining pattern [42]. In *M. rosenbergii*, the MAP1LC3 and SQSTM1 proteins were detected in the gonad by IHC [10].

The results showed that autophagy is constitutively detected at both the molecular and protein levels in the tested tissues of the Pacific oyster. Several studies have already reported that autophagy is implicated in a variety of cellular processes like innate immunity, response to environmental stressors (like anoxia and hyperthermia), and embryonic and larval development in mollusks [11,12,15,16,44]. However, in *C. gigas*, the cellular functions of autophagy need to be further investigated.

Materials and methods

Identification of autophagy proteins in C. gigas

A preliminary search for *C. gigas* ATG homologs was performed in Uniprot (https://www.uniprot.org/). As a second approach, we used the tBLASTn program of NCBI (https://www.ncbi.nlm.nih.gov/) to search for *H. sapiens* (taxid: 9606)

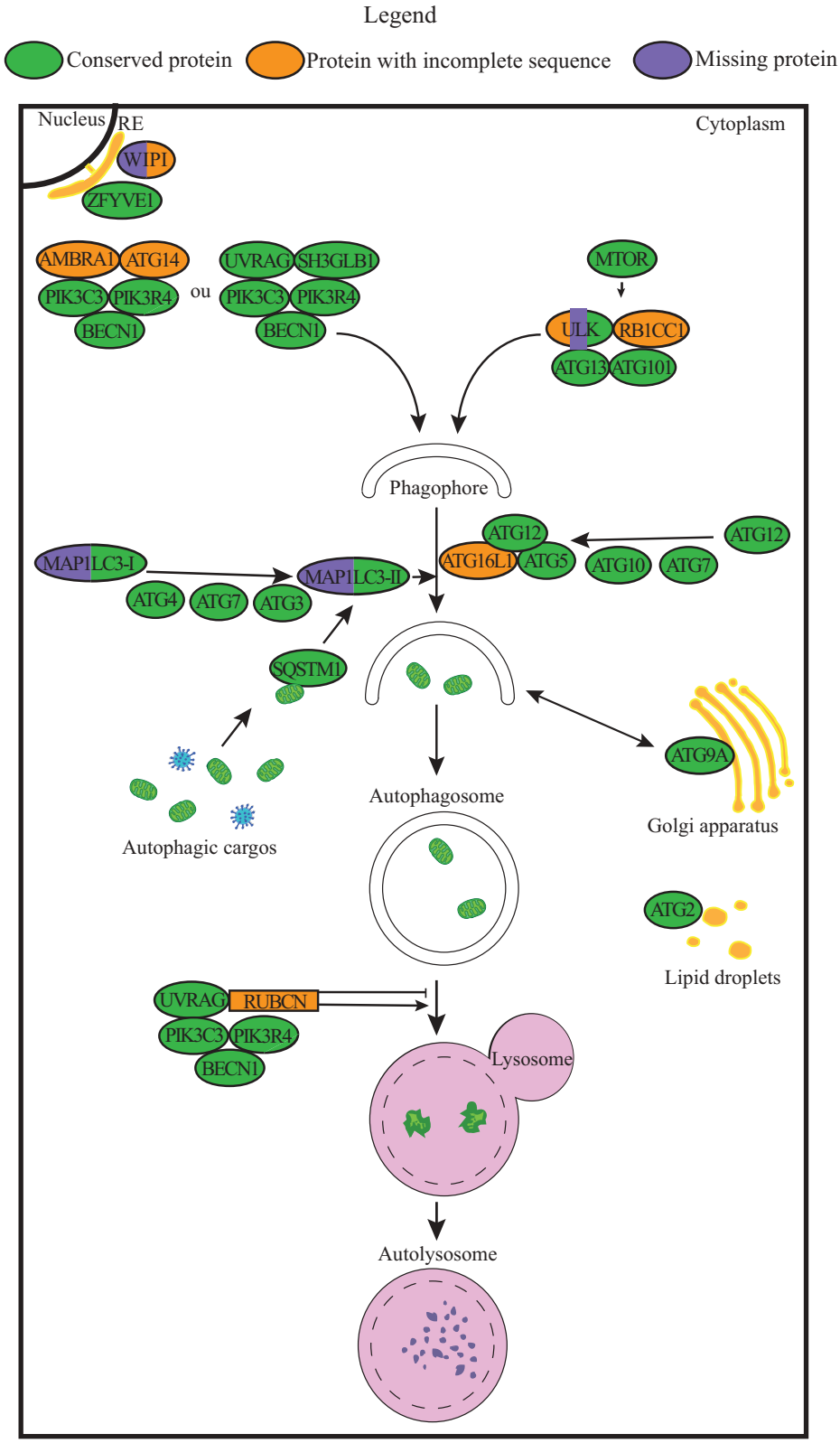

Figure 8. Molecular and cellular autophagy pathway of the Pacific oyster, *Crassostrea gigas*. RE, reticulum endoplasmic.

and *S. cerevisiae* (taxid: 4932) *ATG* homologs using *C. gigas* ATG protein sequences collected from the Uniprot database. For ATG only present in *S. cerevisiae* and *H. sapiens* or not found in *C. gigas* by other approaches, we used the tBLASTn program of NCBI to search for *C. gigas* (taxid: 29,159) *ATG* homologs using *H. sapiens* and *S. cerevisiae* reviewed ATG protein sequences collected from the Uniprot database. The percent identity of each *C. gigas* ATG sequence with the human and yeast sequences was collected. Conserved domain analysis of each *C. gigas* ATG was performed using the

conserved domains-search module of NCBI. All the protein sequences of the 3 organisms are provided in Supplementary file n°1 (Fig. S1).

Statistical analysis

For the identification of ATG proteins in *C. gigas* by the different approaches described in the previous paragraph, the e-value parameter was set at 10^{-5} for selecting significant ATG homolog sequences of *C. gigas, H. sapiens* or *S. cerevisiae*.

Oysters

One-year-old Pacific oysters, *C. gigas*, were produced at the Ifremer facilities in Argenton, Finistère, France. Animals were maintained in raceways supplied with a constant flow of seawater at 19°C, enriched in phytoplankton (*Skeletonema costatum, Isochrysis galbana*, and *Tetraselmis suecica*) cultivated at the Ifremer facilities in Argenton.

Total RNA extraction and cdna synthesis

Pieces of mantle, gills, labial palps, muscle, digestive gland, heart, and gonad were collected from Pacific oysters (100 mg). A 1-mL pool of hemolymph was withdrawn from the adductor muscle of 4 animals.

For each tissue, total ribonucleic acid (RNA) was extracted using TRIzol™ Reagent (Ambion, 15596026) according to the manufacturer's recommendations. Total RNA was treated with TURBO™ DNAse (Invitrogen, AM2238) to remove genomic deoxyribonucleic acid (DNA). The quality and quantity of the RNA were determined using a NanoDrop 2000 (Thermo Scientific, USA). A mock reverse transcription was performed after each DNAse treatment to control for the absence of oyster and/or viral genomic DNA. First-strand cDNA synthesis was carried out using SuperScript® III Reverse Transcriptase (Invitrogen, 18080044) with 500 ng of treated RNA.

Identification and characterization of ATG genes

To obtain full-length cDNAs for *ATG7, ATG12* and *ATG9*, RACE-PCR reactions were carried out using the SMARTer® RACE 5′/3′ Kit (Takara bio, 634859) according to the manufacturer's instructions. Primers were designed using the open-source Primer3 software (http://biotools.umassmed.edu/bioapps/primer3_www.cgi) and synthesized by Eurogentec (Table 6). First-strand cDNAs synthesis, ligation, and cloning were performed with the TA Cloning Kit (Invitrogen, K202020) and transformation was performed with One Shot™ TOP10 Chemically Competent *Escherichia coli* (Invitrogen, C404003). Several clones were sequenced from both ends using the BigDye® Terminator v3.1 sequencing kit (Applied Biosystems, 4337456) with an ABI PRISM® 3130 XL-Avant Genetic Analyzer (Applied Biosystems', USA), a 36 cm capillary array (Applied Biosystems, 4315931), and POP 7 polymer (Applied Biosystems, 4352759). ORFs and protein conserved domains were identified (ORF finder and conserved domain, NCBI). Complete sequences were deposited in GenBank and assigned under the accession numbers MK069430 (*ATG9*), MK069431 (*ATG12*), and MK173046 (*ATG7*). The isoelectric point and molecular mass were calculated in http://www.expasy.ch/tools/pi_tool.html.

Protein sequence alignment and phylogenetic analysis

Multiple amino acid sequence alignments were performed with sequences from 10 species: human (*H. sapiens*), eastern oyster (*Crassostrea virginica*), chicken (*Gallus gallus*), zebrafish (*Danio rerio*), fly (*Drosophila melanogaster*), worm (*Caenorhabditis elegans*), mouse (*Mus musculus*), sea urchin (*Strongylocentrotus purpuratus*), lamp shell (*Lingula unguis*), and European honey bee (*Apis mellifera*). The ATG protein sequences of the ten species were obtained from the Uniprot or NCBI databases. Alignments were performed using ClustalW [45] with the BioEdit sequence alignment editor version 7.0.5.3 (Hall North Carolina state University, USA). The phylogenetic trees were constructed with MEGA 7 software version 7.0.26 (Temple University, King Abdulaziz University and Tokyo Metropolitan University; USA, Saudi Arabia, Japan) using the Neighbor joining method (bootstrap = 1000). The amino acid sequences from the ten species used to perform the alignments and the phylogenetic analysis are listed in supplementary file n°2 (Fig. S2).

Real-time quantitative PCR and relative expression

Real-time quantitative PCR was performed in duplicate using an Mx3000 Thermocycler sequence detector (Agilent, USA). All forward and reverse primers used in the present study were designed using Primer3 software (http://biotools.umassmed.edu/bioapps/primer3_www.cgi) and synthesized by Eurogentec. Real-time quantitative PCR was used to evaluate *ATG* gene expression (*ATG12, ATG9, BECN1, MAP1LC3A, MTOR*, and *SQSTM1*). Amplification reactions were performed in a total volume of 20 µL. Each well contained 5 µL cDNA (diluted 1:30), 10 µL Brilliant III Ultra-Fast SYBR® green qPCR Master Mix (Agilent, 600882), 2 µL of each primer (3 µM) and 1 µL distilled water. The cycling conditions were as follows: 3 min at 95°C, followed by 40 cycles of amplification at 95°C for 5 s and 60°C for 20 s. Melting curves were also plotted to ensure that a single PCR product was amplified for each set of primers. In all cases, negative controls (without cDNA) were included to rule out DNA contamination.

Four specific primer pairs were designed for unique gene sense or antisense sequences and validated by real-time PCR (Table 7). Standard curves were generated for each primer pair using serial dilutions of total cDNA, and PCR efficacy ($E = 10^{(-1/slope)}$) was calculated based on these curves [46]. Thus, the 6 *ATG*s were normalized using the oyster housekeeping gene of *C. gigas, EEF1A1/EF1-α* (eukaryotic translation elongation factor 1 alpha 1; GenBank, Accession N°. AB122066). A pool of the different tissues of *C. gigas* tested in this experiment was used for calibration. The relative quantification value (ratio R) was calculated using the method described by Pfaffl, 2001 [47]: $R = [(E_{target})^{\Delta CT\ target(control\text{-}sample)}]/[(E_{ref})^{\Delta CT\ ref(control\text{-}sample)}]$. All amplification obtained by real-time PCR was validated by sequencing using

Table 7. List of the oyster housekeeping and autophagy genes targeted by real-time PCR.

Gene name	Abbreviation	Forward primer	Reverse primer	Efficiency (%)
Microtubule associated protein 1 light chain 3 alpha	*MAP1LC3A*	CCGATGCTTGACAAGACCAA	CCGTCCTCGTCTTTCTCCTG	98.2
Beclin 1	*BECN1*	AAATGCTGCTTGGGGTCAGA	CGGAATCCACCAGACCCATA	102.2
Mechanistic target of rapamycin kinase	*MTOR*	GGCATGTTCTCTACCCTGGA	TCCTTGACGTTCTCTGACCT	106.7
Sequestosome 1	*SQSTM1*	AGGGAATGAGAAGGCCGAAA	CCTCAAGCAACTCCTCTCCA	96.5
Autophagy related 9	*ATG9*	CTCCTGATTGGTCAGGCAAT	ACGCAGGGAAAAGCAGAGTA	100
Autophagy related 12	*ATG12*	GGGGTTAACCACAAGAAGCA	ACCAAGAGCCATCCATCAAC	100
Eukaryotic translation elongation factor 1 alpha 1	*EEF1A1/EF1-α*	AGTCACCAAGGCTGCACAGAAAG	TCCGACGTATTTCTTTGCGATGT	98.8

the ABI PRISM® 3130 XL-Avant Genetic Analyzer with a 36 cm capillary array and POP 7 polymer (data not shown).

Western blotting

Pieces of mantle, gills, labial palps, muscle, digestive gland, heart, and gonad were collected from one Pacific oyster (20 to 25 mg). A pool of 10 mL of hemolymph from 12 animals was withdrawn from the adductor muscle and centrifuged for 10 min at 1500 × g at 4°C. The supernatant was discarded, and the pellet containing the hemocytes was used for protein extraction.

For each tissue sample, protein extraction was carried out in 200 µL cell extraction buffer (Invitrogen, FNN0011). Samples were ground using a pellet piston and lysed on ice for 30 min in cell extraction buffer with 1 mM phenylmethylsulfonyl fluoride (PMSF; Euromedex, S3025) supplemented with a protease inhibitor cocktail (GE Healthcare, 80-6501-23). Lysates were centrifuged at 13,000 x g for 10 min at 4°C, and supernatant fractions were recovered. All the extracted samples were quantified using the commercial Pierce™ BCA protein assay kit (Thermo Scientific, 23227).

From each tissue, 30 µg of protein extract was loaded and migrated on an 8-16% sodium dodecyl sulfate (SDS)-polyacrylamide gel (Bio-Rad, 4561103). For hemocytes, only 22 µg was loaded. Proteins were transferred onto a polyvinylidene difluoride (PVDF) membrane (Bio-Rad, 1620177) and blocked in TBST 5% BSA (Tris-buffered saline [TBS; Euromedex, ET220], 0.1% Tween 20 [Euromedex, 2001-B], 5% bovine serum albumin [BSA; Sigma-Aldrich, A7906]) for 45 min. The membrane was then incubated overnight at 4°C with the following primary antibodies: MAP1LC3 at 1:200 (Cell Signaling Technology, 4108), BECN1 at 1:1000 (Cell Signaling Technology, 3738), MTOR at 1:1000 (Thermo Fisher Scientific, PA5-13263), ACT/actin at 1:500 (Sigma-Aldrich, A4700), and SQSTM1 at 1:6000 (Sigma-Aldrich, P0067), diluted in TBST 5% BSA. The ACT antibody was used as a loading control. Membranes were washed 3 times for 10 min at room temperature with TBST 1% BSA (Tris-buffered saline [TBS], 0.1% Tween 20, 1% BSA). Membranes were then incubated with horseradish peroxidase (HRP)-conjugated secondary antibodies (anti-rabbit at 1:2500, GE Healthcare, NA934; or anti-mouse at 1:5000, GE Healthcare, NA931) for 45 min at room temperature. Each membrane was washed 3 times for 10 min with TBST 1% BSA. Immunoreactive bands were then detected by enhanced chemiluminescence using the amersham ECL western blotting analysis system (GE Healthcare, RPN2109).

Immunohistochemistry

Whole oysters were preserved in Davidson's fixative (22% formaldehyde [VWR International, 20910.363], 33% ethanol 95% [VWR International, 20824.365], 12% glycerol [VWR International, 24388.364], 33% filtered sea water [0.2-µm filters, Millipore, MILFSVGV01015], and 10% acetic acid [VWR International, 20103.364]) for 48 h and then stored in ethanol before being embedded in paraffin wax blocks. Sections 5 µm thick were cut and mounted on silane-coated slides (Dutscher, 100003). The tissues were deparaffinized in xylene twice for 10 min, rinsed twice for 10 min with absolute ethanol, and unmasked in citrate buffer (0.1 M, pH 6, Sigma-Aldrich, C0759) for 30 min at 90°C. After cooling, slides were washed in 1X phosphate-buffered saline (PBS; Euromedex, ET330) for 10 min. Nonspecific binding was blocked using PBS containing 1% dried skimmed milk (Dutscher, 711160), for 30 min at ambient temperature. The slides were then incubated overnight at 4°C with the polyclonal primary antibody diluted in 1X PBS, supplemented with 0.5% dried skimmed milk (1:10 for anti-MTOR [Thermo Scientific, PA5-13263]; 1:20 for anti-MAP1LC3A [Abgent, AP1805a]; 1:100 for anti-SQSTM1 [Sigma-Aldrich, P0067]; 1:50 for anti-BECN1 [GeneTex, GTX55535]). Unbound primary antibodies were removed with 5 washes in PBS 1X. The slides were then incubated for 45 min with the secondary anti-rabbit antibody (Sigma-Aldrich, A0545) diluted 1:200 in 1X PBS supplemented with 0.5% dried skimmed milk at ambient temperature in the dark. Unbound secondary antibody was removed with 5 washes in 1X PBS in the dark.

Using the SIGMAFAST™ 3,3′-diaminobenzidine (DAB) tablet set (Sigma-Aldrich, D4168), one 3,3′-diaminobenzidine tablet and one urea-hydrogen peroxide tablet were dissolved in 1 mL of water. This solution was added to each tissue section, and the sections were then incubated for 10 min in the dark at room temperature. The reaction was stopped by rinsing the slides with distilled water. Sections were stained for 10 s in Mayer hematoxylin (VWR International, 10047105), then 30 s in water, 1 min in absolute ethanol, and finally soaked in xylene before mounting with Eukitt resin (VWR International, SIAM03989) for microscopic observation. For negative controls, the same protocol was used but without adding the primary antibodies.

Disclosure statement

No potential conflict of interest was reported by the authors.

Funding

This work received financial support from the European project VIVALDI (H2020 n°678589). The region Poitou-Charentes, France and Ifremer support these research works.

ORCID

Isabelle Arzul http://orcid.org/0000-0001-5436-5927

References

[1] Glick D, Barth S, Macleod KF. Autophagy: cellular and molecular mechanisms. J Pathol. 2010;221(1):3–12.
[2] Mizushima N, Yoshimorim T, Levine B. Methods in mammalian autophagy research. Cell. 2010;140(3):313–326.
[3] Ohsumi Y. Historical landmarks of autophagy research. Cell Res. 2014;24(1):9–23.
[4] Kuma A, Komatsu M, Mizushima N. Autophagy-monitoring and autophagy-deficient mice. Autophagy. 2017;13(10):1619–1628.
[5] Yang Z, Klionsky DJ. An overview of the molecular mechanism of autophagy. Curr Top Microbiol Immunol. 2009;335:1–32.
[6] Suzuki H, Osawa T, Fujioka Y, et al. Structural biology of the core autophagy machinery. Curr Opin Struct Biol. 2017;43:10–17.
[7] Yang Z, Klionsky DJ. Mammalian autophagy: core molecular machinery and signaling regulation. Curr Opin Cell Biol. 2010;22(2):124–131.
[8] Zhou X-M, Zhao P, Wang W, et al. A comprehensive, genome-wide analysis of autophagy-related genes identified in tobacco suggests a central role of autophagy in plant response to various environmental cues. DNA Res. 2015;22(4):245–257.
[9] Xie Z, Klionsky DJ. Autophagosome formation: core machinery and adaptations. Nat Cell Biol. 2007;9(10):1102–1109.
[10] Suwansa-Ard S, Kankuan W, Thongbuakaew T, et al. Transcriptomic analysis of the autophagy machinery in crustaceans. BMC Genomics. 2016;17:587.
[11] Bai R, You W, Chen J, et al. Molecular cloning and expression analysis of GABA(A) receptor-associated protein (GABARAP) from small abalone, Haliotis diversicolor. Fish Shellfish Immunol. 2012;33(4):675–682.
[12] Moreau P, Moreau K, Segarra A, et al. Autophagy plays an important role in protecting Pacific oysters from OsHV-1 and vibrio aestuarianus infections. Autophagy. 2015;11(3):516–526.
[13] Barbosa-Solomieu V, Renault T, Travers M-A. Mass mortality in bivalves and the intricate case of the Pacific oyster, Crassostrea gigas. J Invertebr Pathol. 2015;131:2–10.
[14] Zhang G, Fang X, Guo X, et al. The oyster genome reveals stress adaptation and complexity of shell formation. Nature. 2012;490(7418):49–54.
[15] Balbi T, Cortese K, Ciacci C, et al. Autophagic processes in Mytilus galloprovincialis hemocytes: effects of Vibrio tapetis. Fish Shellfish Immunol. 2018;73:66–74.
[16] Moore MN, Viarengo A, Donkin P, et al. Autophagic and lysosomal reactions to stress in the hepatopancreas of blue mussels. Aquat Toxicol. 2007;84(1):80–91.
[17] Sforzini S, Moore MN, Oliveri C, et al. Role of mTOR in autophagic and lysosomal reactions to environmental stressors in molluscs. Aquatic Toxicol. 2018;195:114–128.
[18] Wirawan E, Lippens S, Vanden Berghe T, et al. Beclin1: a role in membrane dynamics and beyond. Autophagy. 2012;8(1):6–17.
[19] Yeh -Y-Y, Shah KH, Herman PK. An Atg13 protein-mediated self-association of the Atg1 protein kinase is important for the induction of autophagy. J Biol Chem. 2011;286(33):28931–28939.
[20] Ragusa MJ, Stanley RE, Hurley JH. Architecture of the Atg17 complex as a scaffold for autophagosome biogenesis. Cell. 2012;151(7):1501–1512.
[21] Chan EYW, Longatti A, McKnight NC, et al. Kinase-inactivated ULK proteins inhibit autophagy via their conserved C-terminal domains using an Atg13-independent mechanism. Mol Cell Biol. 2009;29(1):157–171.
[22] Lee Y-K, Lee J-A. Role of the mammalian ATG8/LC3 family in autophagy: differential and compensatory roles in the spatiotemporal regulation of autophagy. BMB Rep. 2016;49(8):424–430.
[23] Lamark T, Kirkin V, Dikic I, et al. NBR1 and p62 as cargo receptors for selective autophagy of ubiquitinated targets. Cell Cycle. 2009;8(13):1986–1990.
[24] Komatsu M, Ichimura Y. Physiological significance of selective degradation of p62 by autophagy. FEBS Lett. 2010;584(7):1374–1378.
[25] Komatsu M, Waguri S, Koike M, et al. Homeostatic levels of p62 control cytoplasmic inclusion body formation in autophagy-deficient mice. Cell. 2007;131(6):1149–1163.
[26] Bjørkøy G, Lamark T, Brech A, et al. p62/SQSTM1 forms protein aggregates degraded by autophagy and has a protective effect on huntingtin-induced cell death. J Cell Biol. 2005;171(4):603–614.
[27] Lin X, Li S, Zhao Y, et al. Interaction domains of p62: a bridge between p62 and selective autophagy. DNA Cell Biol. 2013;32(5):220–227.
[28] Wang X, Terpstra EJM. Ubiquitin receptors and protein quality control. J Mol Cell Cardiol. 2013;55:73–84.
[29] Yorimitsu T, Klionsky DJ. Autophagy: molecular machinery for self-eating. Cell Death Differ. 2005;12(Suppl 2):1542–1552.
[30] Klionsky DJ, Schulman BA. Dynamic regulation of macroautophagy by distinctive ubiquitin-like proteins. Nat Struct Mol Biol. 2014;21(4):336–345.
[31] E-J L, Tournier C. The requirement of uncoordinated 51-like kinase 1 (ULK1) and ULK2 in the regulation of autophagy. Autophagy. 2011;7(7):689–695.
[32] Proikas-Cezanne T, Takacs Z, Dönnes P, et al. WIPI proteins: essential PtdIns3P effectors at the nascent autophagosome. J Cell Sci. 2015;128(2):207–217.
[33] Schaaf MBE, Keulers TG, Vooijs MA, et al. LC3/GABARAP family proteins: autophagy-(un)related functions. Faseb J. 2016;30(12):3961–3978.
[34] Russell RC, Tian Y, Yuan H, et al. ULK1 induces autophagy by phosphorylating Beclin-1 and activating VPS34 lipid kinase. Nat Cell Biol. 2013;15(7):741–750.
[35] McAlpine F, Williamson LE, Tooze SA, et al. Regulation of nutrient-sensitive autophagy by uncoordinated 51-like kinases 1 and 2. Autophagy. 2013;9(3):361–373.
[36] Nakatogawa H, Suzuki K, Kamada Y, et al. Dynamics and diversity in autophagy mechanisms: lessons from yeast. Nat Rev Mol Cell Biol. 2009;10(7):458–467.
[37] Ravikumar B, Sarkar S, Davies JE, et al. Regulation of mammalian autophagy in physiology and pathophysiology. Physiol Rev. 2010;90(4):1383–1435.
[38] Jin S. Autophagy, mitochondrial quality control, and oncogenesis. Autophagy. 2006;2(2):80–84.
[39] Mizushima N, Yoshimori T. How to interpret LC3 immunoblotting. Autophagy. 2007;3(6):542–545.
[40] Mizushima N, Yamamoto A, Matsui M, et al. In vivo analysis of autophagy in response to nutrient starvation using transgenic mice expressing a fluorescent autophagosome marker. Mol Biol Cell. 2004;15(3):1101–1111.
[41] Tanida I, Minematsu-Ikeguchi N, Ueno T, et al. Lysosomal turnover, but not a cellular level, of endogenous LC3 is a marker for autophagy. Autophagy. 2005;1(2):84–91.
[42] Klionsky DJ, Abdelmohsen K, Abe A, et al. Guidelines for the use and interpretation of assays for monitoring autophagy (3rd edition). Autophagy. 2016;12(1):1–222.
[43] Martinet W, Roth L, De Meyer GRY. Standard immunohistochemical assays to assess autophagy in mammalian tissue. Cells. 2017;6:3.
[44] Moore MN. Autophagy as a second level protective process in conferring resistance to environmentally-induced oxidative stress. Autophagy. 2008;4(2):254–256.

[45] Thompson JD, Gibson TJ, Plewniak F, et al. The CLUSTAL_X windows interface: flexible strategies for multiple sequence alignment aided by quality analysis tools. Nucleic Acids Res. 1997;25(24):4876–4882.
[46] Rasmussen R. Quantification on the LightCycler. In: Meuer S, Wittwer C, Nakagawara K-I, editors. Rapid cycle real-time PCR: methods and applications. Berlin, Heidelberg: Springer Berlin Heidelberg; 2001. p. 21–34.
[47] Pfaffl MW. A new mathematical model for relative quantification in real-time RT-PCR. Nucleic Acids Res. 2001;29(9):e45.